# NEW FEATURES IN SUPERDEFORMED NUCLEI*

M.A. DELEPLANQUE

Nuclear Science Division, Lawrence Berkeley Laboratory
Berkeley CA, 94720, USA

*(Received November 15, 1994)*

New features in superdeformed nuclei observed with the new generation of large gamma-ray detector arrays are presented. The first part gives for the first time a microscopic scenario for the decay of a superdeformed band in the mass 130 region. The second part presents experimental evidence for a new type of symmetry, namely $C_4$ symmetry, in superdeformed nuclei. A phenomenological study of how the staggering occurs for a $Y_{44}$ deformation is discussed.

PACS numbers: 21.10. Re, 21.60. Ev, 23.20. Lv, 27.60. +j

## 1. Introduction

In this talk, I want to present new features in superdeformed (SD) nuclei that have been possible to observe only with the new generation of $\gamma$-ray detector arrays. SD nuclei are stable when there is a "second minimum" at large deformation in a potential-energy curve as a function of the deformation (elongation) parameter. Their existence is due to "gaps" in the single-particle energy curves that occur at large deformation for certain nucleon numbers. Also the resulting large moment of inertia favors these large deformations at high spins as compared to lower deformation, producing the second minimum. However, the population in that minimum is in general weak in Heavy-Ion reactions (typically $\sim$ 1 % of the cross section of a residual nucleus produced). Therefore to observe such detailed and weak features as the links between the SD band and the low-lying states, or very precise energies, one needs very powerful $\gamma$-ray detector arrays. The resolving power of the various generations of arrays (see Stephens, this conference) is a measure of their performance. Thus, the intensity of the weakest resolvable branch in a nucleus decreases roughly from 1 % in previous generation

* Presented at the XXIX Zakopane School of Physics, Zakopane, Poland, September 5–14, 1994.

detector systems such as HERA to 0.1 % in the present detector systems such as the Early Implementation (EI) of Gammasphere, or Eurogam I, or GASP, to 0.01 % in the arrays which will be used in the near future, such as the final Gammasphere or Euroball III. I will talk about features observed with the present detector systems, namely the EI of Gammasphere. We observed the linking transitions of $^{135}$Nd down to a few percent of the SD band intensity. With the rather good statistics obtained for three- and four-(clean Ge)fold coincidences, we could measure precise $\gamma$-ray energies and see in some nuclei small deviations from smooth values that are intriguing.

## 2. The decay of the SD band in $^{135}$Nd

The SD band in $^{135}$Nd was observed in 1987 [1] and already then, some linking transitions were proposed but I think it is fair to say that there was a general disbelief that the proposed transitions were the links. With the aim of finding the full decay pattern of the SD band, we used the reactions $^{40}$Ar+$^{100}$Mo at 182 and 176 MeV at the EI of Gammasphere, with 24 and 36 detectors respectively [2]. We could use the power of the array to obtain clean spectra from three-fold data.

### *2.1. The SD band*

Fig. 1 shows a spectrum of the band, double gated on all combinations of the SD lines (except the 602 keV line) up to 1215 keV. Four new lines are seen (marked by arrows) that continue the decreasing trend of the moment of inertia (see Fig.2). This regularity suggests that the structure of the band does not change (i.e its configuration, pairing properties) and the decrease means that angular momentum becomes more difficult to generate as more and more of the orbits become aligned.

### *2.2. The decay pattern*

To find the linking transitions between the SD band and the low-deformation states, one needs very clean spectra so that the real (very weak) transitions could not just be contaminants. Therefore the method is to construct a matrix gated on the only four clean (background subtracted) lines of the SD band. By putting a second gate on a particular low-lying transition, one enhances the path between the SD band and the state depopulated by that transition. Figs 3 shows such spectra and the resulting level scheme for the decay is shown in Fig.4. The previous lines proposed are confirmed and a number of new lines are also placed, amounting to about 63 % of the intensity of the SD band.

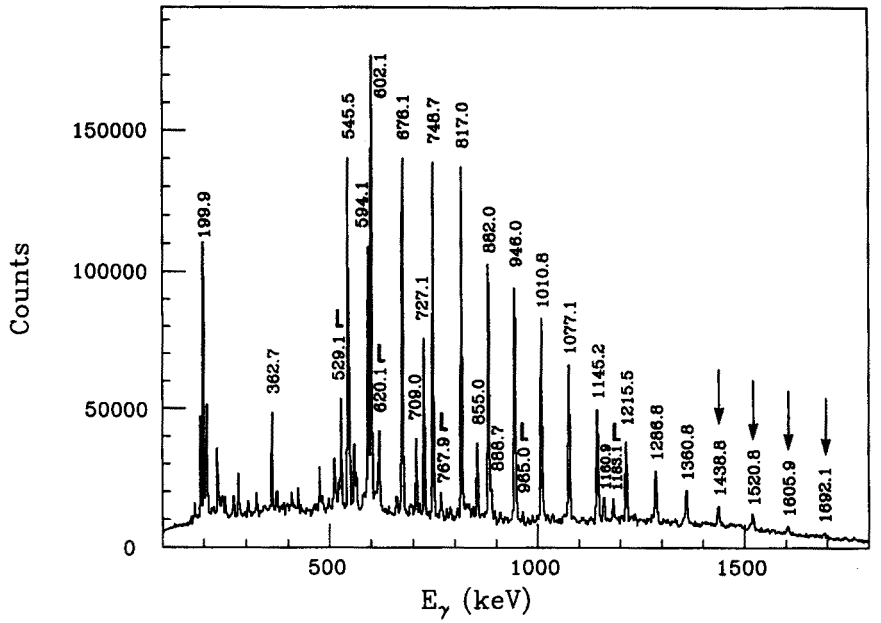


Fig. 1. Triple-coincidence gamma-ray spectrum of the SD band obtained in $^{135}$Nd at 182 MeV (see text). The new lines are marked by arrows and some visible linking transitions are marked by an "L". Some yrast transitions are also seen.

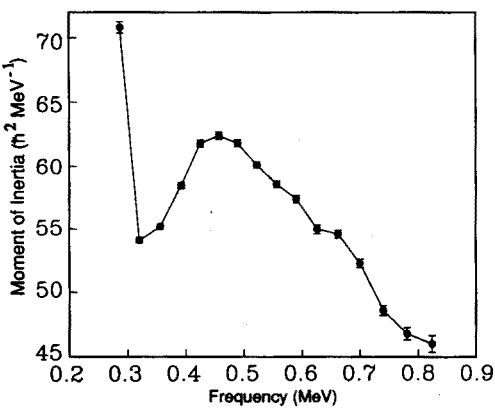


Fig. 2. Dynamic moment of inertia for the SD band of $^{135}$Nd.

For the experiment at 176 MeV, there were six detectors at 90°, so that angular correlation data could be obtained. Two spectra, gated by the clean SD lines in the forward and backward directions (and background subtracted), were generated at the forward-backward angles ($\theta_{\mathbf{ave}} \sim 28°$) and at 90°. Because of the axial symmetry around the beam direction for

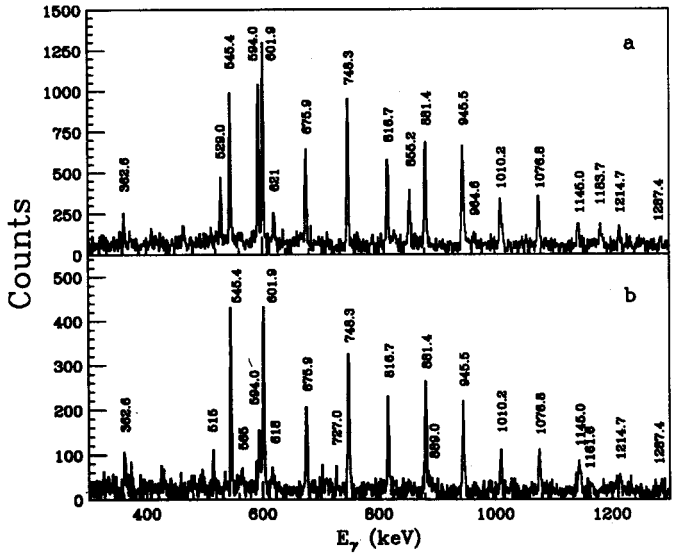


Fig. 3. Triple-coincidence spectra showing some linking transitions between the SD band and the yrast states in $^{135}$Nd. In these spectra, one gate was set on any of the four clean lines in the SD band (*i.e.*, 676, 817, 1010 and 1145 keV) and the other gate was set on (a) the 727 keV line and (b) the 549 keV line.

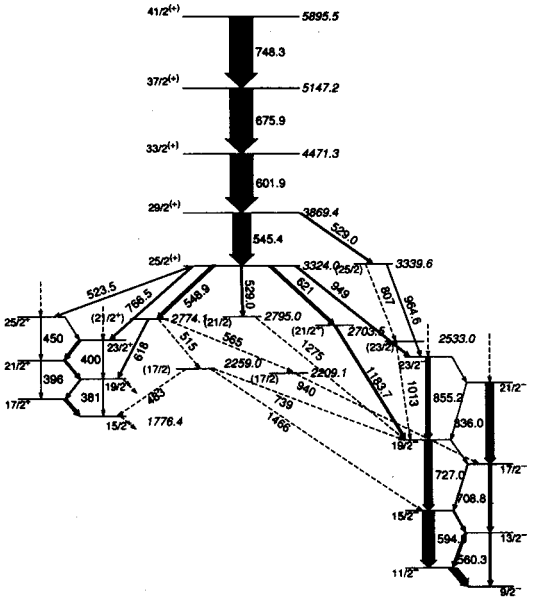


Fig. 4. Lower part of the level scheme of $^{135}$Nd, showing the lower states of the SD band, the lower part of the previously known normally deformed states, and the newly established decay pattern of the SD band into them. The widths of the lines represent the measured $\gamma$-ray intensities. The transitions represented by a dashed line are tentative.

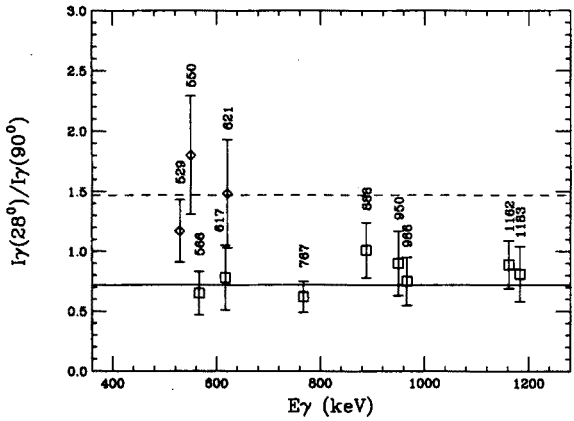


Fig. 5. "Angular correlations" for some linking transitions and some other known transitions. The ratio (28°/90°) of $\gamma$-ray intensities is determined from spectra gated by the clean SD lines at 676 and 817 keV in the forward and backward detectors and background subtracted. The solid and dashed lines represent an average value of this ratio measured for known stretched quadrupole and stretched dipole transitions respectively.

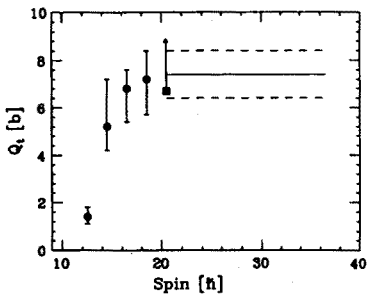


Fig. 6. Transition quadrupole moments $Q_t$ for E2 transitions with energies (from left to right) 621, 545, 602, 676 and 748 keV obtained from the RDM measurement [4]. The lines give the average quadrupole moments and uncertainties for the higher spin transitions from the DSAM measurement [3].

the SD gates, the intensity of the lines in these two spectra corresponds to that of an angular distribution relative to the beam direction. The ratio of intensities at 28° and 90° is shown in Fig. 5 for the most intense linking transitions as well as a few other low-lying lines not known before. The solid and broken lines represent averages obtained with these same spectra for lines of known multipolarity. The multipolarities are rather clear for the transitions shown, except for the 529 keV transition which has an intermediate ratio. This may be due to the fact that the 529 keV line is

a doublet. From the level scheme and the multipolarity, one can deduce unambiguously the spins of the SD band but not the parity. However, the spins are consistent with the signature of the $i_{13/2}$ neutron which is the expected configuration. This would imply a positive parity.

### *2.3. Disappearance of the SD band at low spins*

The lifetimes in the SD band have been measured [3] by DSAM and indicate a rather large deformation ($\varepsilon = 0.32$). At the bottom of the SD band and for some linking transitions, longer lifetimes have been measured using the RDM [4]. Fig. 6 gives the RDM resulting transition moments $Q_t$. The values agree with the DSAM values within the band but there is a slight decrease for the moment of the $29/2^+ \rightarrow 25/2^+$ 545 keV transition which could only be measured with the RDM method since this line was stopped in the DSAM measurement. For the next lower E2 transition (*e.g.*, the 620 keV transition), however, $Q_t$ is down by a factor around 25 compared to the value in the SD band. This means that this (620 keV) transition does not belong to the SD band. In the same way, no other transition seen deexciting the $25/2^+$ state belongs to the SD band. If there were a transition continuing the band, we should see a transition of about 500 keV deexciting the $25/2^+$ state with full intensity. We conclude that the SD band "disappears" at the $25/2^+$ level.

### *2.4. The decay mechanism*

To understand what happens at the bottom of the band, Frauendorf performed "ultimate cranker" [5] calculations (cranked modified oscillator with pairing and particle number projection) in which the neutron configuration always includes one $i_{13/2}$ neutron. Total Routhian Surfaces (Fig. 7) show that the minimum at $\hbar\omega = 0.25$ MeV, which is located at $\varepsilon \sim 0.3$ and $\gamma \sim 8°$, is the lowest. It represents the SD band. For $\hbar\omega = 0.15$ MeV the less deformed triaxial minimum ($\varepsilon$ =0.22, $\gamma \sim 30°$) is lower in energy. Between $\hbar\omega = 0.2$ MeV and 0.15 MeV both minima have the same energy with a small barrier between them. We suggest that with decreasing frequency the nucleus slides over from the high-deformation to the low-deformation minimum, resulting in the observed band termination.

The change in configuration between the two minima can be understood by looking on Fig. 8 at the single-particle energies as a function of $\gamma$ along the deformation path indicated at $\hbar\omega = 0.2$ MeV. The second minimum arises from the gap that develops at large triaxiality $\gamma$ between the $\nu\ g_{7/2}$ orbital and the $\nu\ h_{9/2}$ orbital (Fig. 8, bottom). Thus, as the frequency decreases, the $\gamma$-driving $\nu\ g_{7/2}$ configuration becomes lowest in energy, and the pairing interaction is strong enough to scatter the neutrons from one

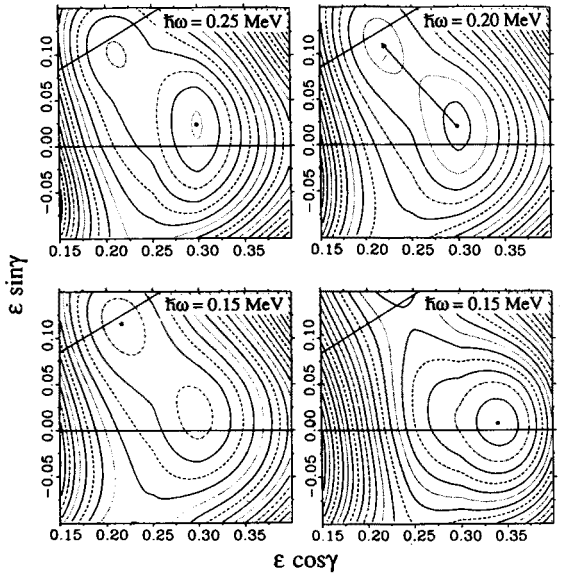


Fig. 7. Total routhian surfaces as a function of deformation $\varepsilon$ and triaxiality $\gamma$ for the neutron $i_{13/2}$ configuration at three different frequencies =0.25, 0.20 and 0.15 MeV in $^{135}$Nd and at $\hbar\omega$=0.15 MeV in $^{133}$Nd (bottom right). The lines corresponding to $\gamma$=0° and $\gamma$=30° are indicated. The contours are separated by 0.2 MeV and the energies of the minima are -1.421, -0.67, -0.097, and -0.319 MeV respectively.

configuration to the other and induce the transition. The effect is similar, although less clear, for the protons where there is a $g_{7/2} \leftrightarrow h_{11/2}$ transition involved. The configuration in the lower deformation minimum differs from the ground configuration by only one neutron ($\nu i_{13/2}$ instead of $\nu\ h_{11/2}$) and it is therefore easy to decay towards the low-lying states. There are also other proton states easily reachable and this explains why the band also decays toward the positive parity states.

This scenario is consistent with the $Q_t$ observed. If we assume that the $29/2^+$ state is superdeformed with $\varepsilon \sim 0.3$, $\gamma \sim 0°$, that the $25/2^+$ state is a 50 % mixture of the SD and lower deformation ($\varepsilon = 0.2$, $\gamma \sim 30°$) states and that the $21/2^+$ state is a lower deformation state, then $Q_t(29/2^+ \rightarrow 25/2^+)/Q_t(25/2^+ \rightarrow 21/2^+)$ is close to the experimental ratio for $Q_t(545)$ / $Q_t(621)$, *i.e.* $\sim$ 25.

The ultimate cranker calculations (Fig. 7) also account for the observed decay of $^{133}$Nd [6]. In that case, the SD band persists down to $17/2^+$ and the calculation shows that the low-deformation minimum does not develop in the frequency range 0.25 to 0.15 MeV. The reason is that the $g_{7/2}$ neutron pair remains empty since $^{133}$Nd has two fewer neutrons than $^{135}$Nd.

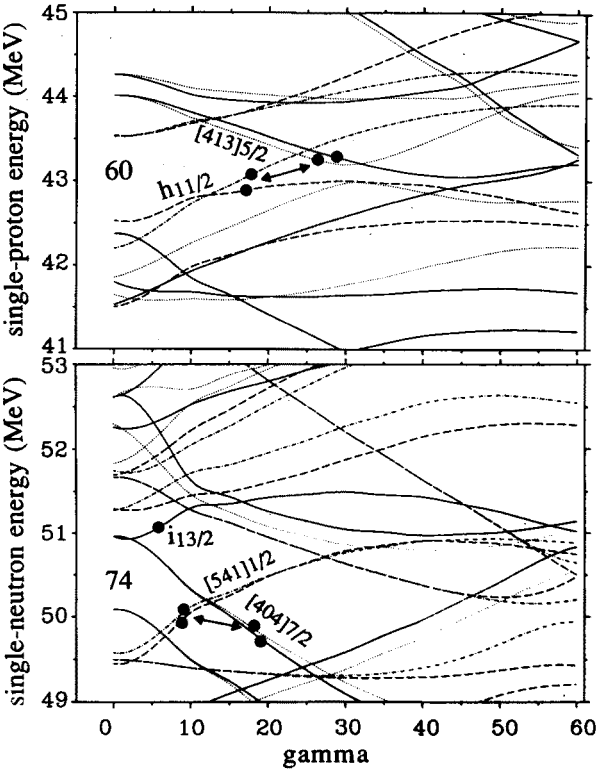


Fig. 8. Single-particle energies as a function of the $\gamma$ deformation at $\hbar\omega = 0.2$ MeV for a variable ($\varepsilon$, $\gamma$) path as indicated in Fig. 4, for (top) protons and (bottom) neutrons. Orbital changes are schematically indicated.

The mechanism proposed for the decay of the SD band of $^{135}$Nd involves an intermediate state with a special configuration that can be called a "doorway state"and triggers the decay of the SD band. In the nucleus $^{135}$Nd, there is only one intermediate configuration and it is possible to follow the decay. A similar mechanism may exist *(i)* below the $17/2^+$ state in $^{133}$Nd, and *(ii)* in many other cases where the "doorway state" could trigger the decay of a SD band, even though it could involve many other steps.

## 3. $C_4$ symmetry in superdeformed nuclei

With the EI of Gammasphere high-statistics high-fold data can be obtained that can give precise $\gamma$-ray energy measurements in SD bands. Fig. 9 shows spectra obtained for the (known) SD bands of $^{194}$Hg [7] in the reaction $^{48}$Ca+$^{150}$Nd at 206 MeV. For band 1, the most intense, we see a quintuple coincidence spectrum between almost all band members, whereas

for bands 2 and 3, these are quadruple coincidence spectra with gates only on the clean lines. These spectra are very clean and on close inspection, the $\gamma$-ray energies show a "staggering" pattern, as indicated on the right part of Fig. 10, rather than the perfect rotational band shown on the left part of the figure. This is called $\Delta I = 2$ staggering and we will discuss later its interpretation in terms of a new $C_4$ symmetry present in the nucleus.

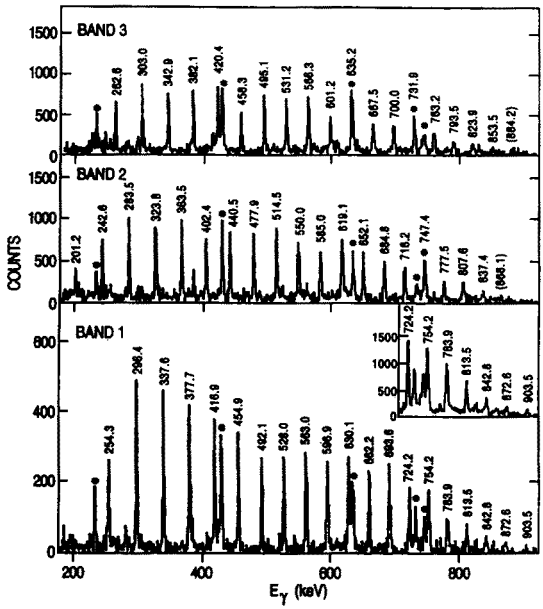


Fig. 9. Gamma-ray spectra of the three SD bands in $^{194}$Hg (see text). The inset shows the highest energy part of band 1 with three gate combinations to confirm the assignment of the 903.5 keV gamma ray.

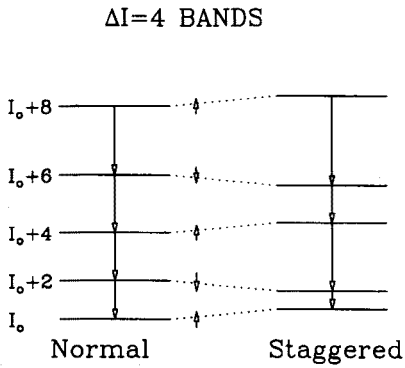


Fig. 10. Schematic representation of a $\Delta I = 2$ "staggered" band (right) compared to that of a normal rotational band (left).

### *3.1. Experimental analysis*

#### 3.1.1. The staggering parameter

In order to quantify this phenomenon, one defines a "staggering parameter" $\Delta E_\gamma(I)$ for each $\gamma$-ray energy $E_\gamma(I)$. It is the deviation from a smooth reference energy which is a quadratic interpolation between $E_\gamma(I)$ and its four neighbors. The expression is:

$$\Delta E_\gamma(I) = \tfrac{3}{8}\left(E_\gamma(I) - \tfrac{1}{6}\left(4E_\gamma(I-2) + 4E_\gamma(I+2) - E_\gamma(I-4) - E_\gamma(I+4)\right)\right), \quad (1)$$

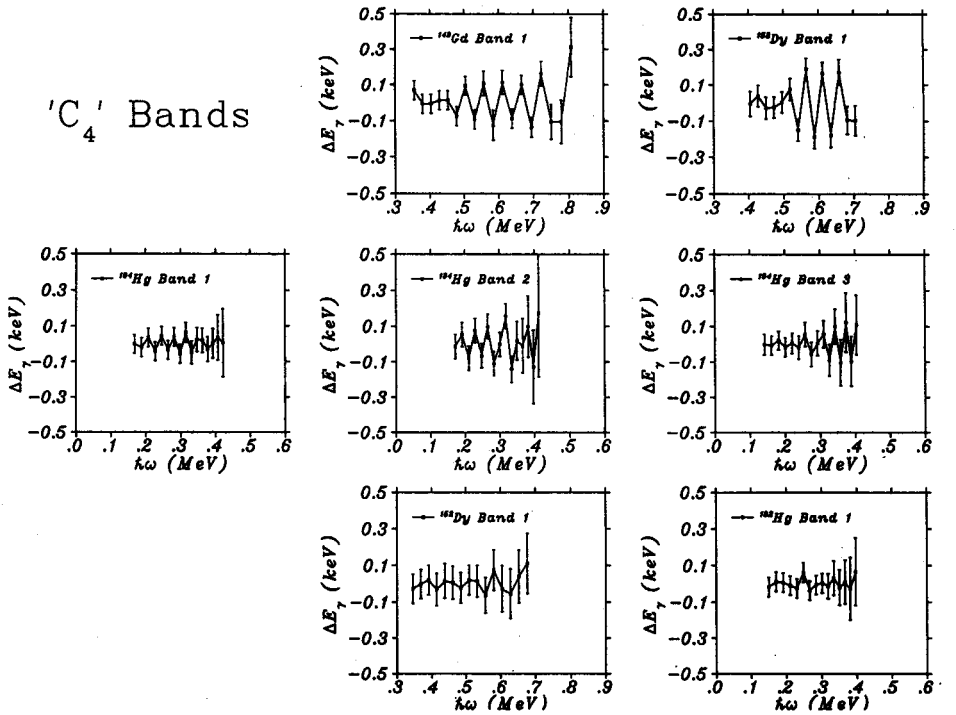


Fig. 11. Staggering parameters as a function of rotational frequency for a variety of SD bands. The two bottom spectra are examples where no staggering effect is found.

Staggering parameters are shown for a number of bands in Fig. 11. The first case of staggering was discovered [8] by a French-Canadian collaboration at Eurogam in $^{149}$Gd. The only other cases found are in $^{194}$Hg [7] and tentatively in the yrast band of $^{153}$Dy [9]. As seen at the bottom of the figure, there are cases [10] of comparable quality which do not show the staggering. In fact, there are rather few SD bands that show it. All the

known cases are shown in Fig. 11. This effect is very small, $\Delta E_\gamma = 100$ eV, which translates into a level shift of $\sim 50$ eV, or of $10^{-4}$ of the transition energy. There are also some restricted ranges where the staggering appears clearer, and in some cases ($^{194}$Hg bands 2 and 3) there is an inversion at the same frequency in the two bands which are thought to be signature partners. Therefore, it is important to ask whether this is or not a real effect.

### 3.1.2. Statistical analysis

Several methods were developed to test the degree of randomness of the observed distributions of staggering parameters. Since, in a perfect case of staggering, the $\Delta E_\gamma$ points stagger every $\Delta$I=2 around zero, if every other point is multiplied by $-1$, the average $\Delta E_\gamma$ should change from 0 to $\Delta E_\gamma$, whereas if the distribution $\Delta E_\gamma$(I) is random, the $\overline{\Delta E_\gamma}$ will remain the same after this transformation. Mathematically, a Gaussian centered at $\overline{\Delta E_\gamma}$ and of width related to the uncertainty on the transition energies can be associated to the experimental distribution of $\Delta E_\gamma$(I). Applying the transformation above, a random distribution will leave the Gaussian unchanged whereas a perfect staggering will displace the Gaussian by $\overline{\Delta E_\gamma}$. Therefore a confidence level C.L. can be defined as the probability that these two Gaussians before and after the transformation do not overlap. The expression for this is:

$$\text{C.L.} = \int_{-\infty}^{+\infty} erf(\Delta E_\gamma, \overline{\Delta E_\gamma}, \sigma) \cdot g(\Delta E_\gamma, \overline{\Delta E'_\gamma}, \sigma') d\Delta E_\gamma \,, \qquad (2)$$

A complete overlap (random distribution) gives C.L. = 0.5, whereas a separation by 1, 2 or 3$\sigma$ gives a C.L. of 0.76, 0.92 and 0.98 respectively. The results are given in column 1 of Table I for some bands of Fig. 11. While the level of confidence is lower for band 3 of $^{194}$Hg, it is rather good for the others.

Another test is to "randomize" the observed $\Delta E_\gamma$ distribution and check if the confidence level of these new distributions is greater than that of the observed one. This can be done in two ways, either *(i)* by "picking" many times at random the order of the observed $\Delta E_\gamma$ values, or *(ii)* by associating a Gaussian (of width the experimental error on $E_\gamma$) to each $\gamma$-ray energy and picking many times at random new values of $E_\gamma$ within each Gaussian. Then in each case, the above statistical analysis is repeated. The probabilities that these "randomized" distributions have a confidence level higher than the experimental ones is given in columns 2 and 3 of Table I. Again from these results we are rather confident that bands 1 and 2 in $^{194}$Hg exhibit a $\Delta$I=2 staggering.

TABLE I

Confidence levels (column 1) and probabilities of no staggering (columms 2 and 3) from randomization tests (see text).

| | Level of confidence | Probability random $\Delta E_\gamma$ | Probability random $\Delta E_\gamma$ |
|---|---|---|---|
| $^{149}$Gd | 0.97 | 0.11 | 0.01 |
| $^{194}$Hg | | | |
| Band 1 | 0.80 | 0.01 | 0.23 |
| Band 2 | 0.82 | 0.09 | 0.19 |
| Band 3 | 0.62 | 0.59 | 0.65 |

### *3.2. Discussion in terms of $C_4$ symmetry*

In analogy with the ΔI=1 staggering which is related to the existence of a $C_2$ symmetry (invariance of the wave function in a rotation of 180°), the $\Delta I = 2$ staggering is proposed to be related to a $C_4$ symmetry (invariance of the wave function in a rotation of 90°).

#### 3.2.1. Axis of symmetry

We know that the SD nuclei rotate around an axis perpendicular to the symmetry axis that exists for a $Y_{20}$ deformation and that there are large E2 transition moments between $\Delta I = 2$ states. Hamamoto and Mottelson [11] have proposed that the small perturbation (*i.e.* staggering) of the main rotation comes from a $Y_{44}$ deformation around the "symmetry" axis. Such a shape is represented in Fig. 12 on a side view down the "symmetry" (or 3-) axis of the nucleus. There are four equivalent minima at 90° from each other and Hamamoto and Mottelson interpret the staggering as due to a tunneling between the four equivalent minima.

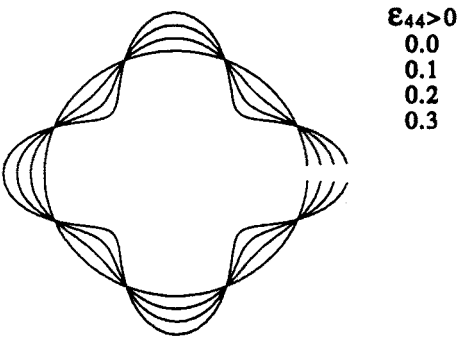


Fig. 12. Cross section of the nucleus perpendicular to the 3-axis showing $Y_{44}$ shapes corresponding to different deformations. $\epsilon_{44}$= 0 corresponds to the spherical shape.

3.2.2. Band mixing approach

We take a slightly different, but equivalent approach [12] in viewing the $Y_{44}$ deformation as restricting the number of excited bands. The nucleus can now "rotate" around the 3-axis, generating a term $A_3K^2$ and the general Hamiltonian can be written as:

$$H_0 = AI^2 + (A_3 - A)K^2, \tag{3}$$

where $A$ is the usual moment of inertia parameter. The condition that the wave function is invariant in a 90° rotation around the 3-axis gives $K = \Omega$, $\Omega \pm 4$, $\Omega \pm 8$, *etc.* and in the following, we will consider $\Omega = 0$. This restricts the possible number of bands to $K = 0, 4...$ but does not produce the staggering. To observe it, the bands need to be mixed, *i.e.*, with fourth-order terms in spin. The most general mixing term can be written:

$$H_c = h_4(I_+^4 + I_-^4) + h_0(I_+^2 I_-^2 + I_-^2 I_+^2 + I_+ I_- I_- I_+ + \ldots), \tag{4}$$

or

$$H_c = h_4(I_+^4 + I_-^4) + h_0(I_+^2 I_-^2 + I_-^2 I_+^2 + 4(I^2 - K^2)^2), \tag{5}$$

where $h_0$ is a diagonal term and $h_4$ a non-diagonal term. This is completely equivalent to the Hamiltonian proposed by Hamamoto and Mottelson

$$H_c = B_1(I_1^2 - I_2^2)^2 + B_2(I_1^2 + I_2^2)^2$$

with $B_1 = 4h_4$ and $B_2 = 2(3h_0 - h_4)$. The $B_1$ term expresses the $C_4$ symmetry around the symmetry axis while the $B_2$ term is axially symmetric. For consistency, we will discuss $H_c$ in terms of $B_1$ and $B_2$ in the following.

3.2.3. Parameters producing the staggering

To find the conditions under which the staggering is produced, Hamamoto and Mottelson considered only the Hamiltonian $H = A_3K^2 + H_c$ since these conditions involve only the ratio $A_3/B_1$. We chose to consider the full Hamiltonian $H = H_0 + H_c$ in order to study the effect on the total moment of inertia and $B(E2)$ which are experimental constraints.

Fig. 13 shows the energy of the yrast states after diagonalization for each spin as a function of the $B_2$ parameter, in units of $I(I+1)$ and for $A = 1$. The $A_3 = 90$ and $B_1 = 1$ parameters are those found by Hamamoto and Mottelson to generate the staggering effect. There are two points that can be made from these results. First, $B_2$ must be equal to zero since only for that value do the various curves converge, which is necessary to find an $I(I+1)$ variation of the energies $E(I)$. Second, $E(I)/I(I+1)$ should be equal to 1 (since we took $A = 1$). Instead we find in this case

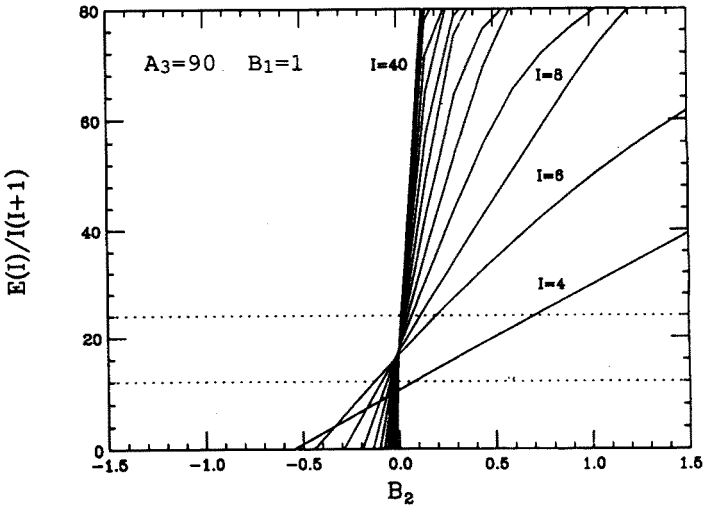


Fig. 13. Total energy, in units of $AI(I+1)$ of the Hamiltonian $H = H_0 + H_c$ as a function of $B_2$ for spins $I = 4$ to 40. The parameters (see text) are $A_3 = 90$, $B_1 = 1$.

$E(I)/I(I+1) \sim 20$ corresponding to a much too small moment of inertia. If we now decrease both $A_3$ ($A_3 = 1.9$) and $B_1$ ($B_1 = 0.01$) while keeping their ratio as before, we find the staggering with a reasonable moment of inertia ($E(I)/I(I+1) = 1.2$) and $B(E2)$ (which is not very much affected).

### 3.2.4. Discussion

Our approach using the full Hamiltonian gave new restricted values of parameters generating the staggering and consistent with the other experimental observables. This approach is based on the hypothesis that the $Y_{44}$ deformation is producing the staggering. However, this assumption is not without problem. In our calculation, we find $A_3 = 1.9$, almost the rigid body value, which is not necessarily what is expected for a small deformation. Microscopic calculations performed by S. Frauendorf assuming a $Y_{44}$ deformation actually do find values of $A_3$ within a factor 2 of our proposed value, but the parameter $B_1$ is found to be 10 times too small to produce the staggering. Whether or not this will turn out to be the correct explanation is not clear. On the experimental side, one needs to look at many more nuclei in hope of characterizing better the conditions under which the staggering occurs. On the theoretical side, more shape degrees of freedom should perhaps be explored.

## 4. Conclusion

I have presented two new features that have been possible to explore only with the new generation of large gamma-ray arrays, here the Early Implementation of Gammasphere. In $^{135}$Nd, we found 63% of the transitions linking the SD band to the normal states, proposed a mechanism for the decay of the band and identified an intermediate configuration. In $^{194}$Hg and perhaps in $^{153}$Dy, we found a $\Delta I = 2$ staggering in some of the SD bands and have explored the possibility that it is related to a new symmetry in the nucleus. Many more studies need to be done to understand these phenomena.

This work has been done with the Nuclear Structure group of the Lawrence Berkeley Laboratory which I would like to acknowledge. I wish to thank particularly B. Cederwall and A.O. Macchiavelli for the discussion of the $C_4$ symmetry, and S. Frauendorf for enlightening discussions and calculations on the decay of superdeformed bands. This work has been supported in part by the Director, Office of Energy Research, Division of Nuclear Physics of the Office of High Energy and Nuclear Physics of the U.S. Department of Energy under Contract Nos. DE-AC03-76SF00098 (LBL) and W-7405-ENG-48 (LLNL).

REFERENCES

[1] E.M. Beck *et al.*, *Phys. Rev. Lett.* **58**, 2182 (1987).
[2] M.A. Deleplanque *et al.*, to be published.
[3] R.M. Diamond *et al.*, *Phys. Rev.* **C41**, R1327 (1990).
[4] P. Willsau *et al.*, *Phys. Rev.* **C48**, R494 (1993).
[5] T. Bengtsson, *Nucl. Phys.* **A496**, 56 (1989).
[6] D. Bazzacco *et al.*, *Phys. Rev.* **C49**, R2281 (1994).
[7] B. Cederwall *et al.*, *Phys. Rev. Lett.* **72**, 3150 (1994).
[8] S. Flibotte *et al.*, *Phys. Rev. Lett.* **71**, 4299 (1994).
[9] B. Cederwall *et al.*, submitted to *Phys. Lett.*
[10] P. Fallon *et al.*, to be published.
[11] I. Hamamoto, B. Mottelson, *Phys. Lett.* **B333**, 294 (1994).
[12] A.O. Macchiavelli *et al.*, submitted to *Phys. Rev.* **C**.